Supplementary Information

Exploration of Ferroelectric Behavior of Turmeric and Its Integration as a Gate Dielectric in Organic Field-Effect Transistors

Ajoy Mandal[1*], Subhamay Pramanik[2], Ishita Jana[3], Sanjoy Satpati[4], Sovanlal Mondal[2], & Kalyan Mandal[3]

[1]Department of Physics, Government General Degree College, Tehatta, 741160, West Bengal, India.

[2]Department of Physics, Indian Institute of Technology Kharagpur, 721302, West Bengal, India.

[3]S. N. Bose National centre for Basic Sciences, JD Block, Sector III, Salt Lake, Kolkata, 700106, India.

[4]Department of Chemistry, Government General Degree College, Tehatta, 741160, West Bengal, India.

Email: ajoymandal989@gmail.com

Supplementary Figure 1

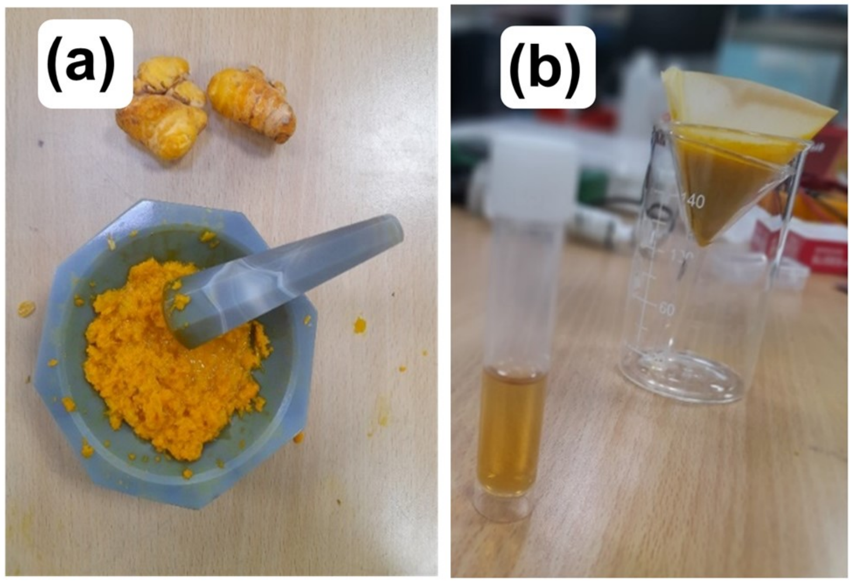

Supplementary Figure S1: Extraction of turmeric juice. (a) Smashed turmeric in a mortar; (b) freshly prepared raw turmeric solution. The solution was subsequently filtered using 0.2 µm pore-size filter paper to remove particulates and obtain a clear extract.

Supplementary Figure 2

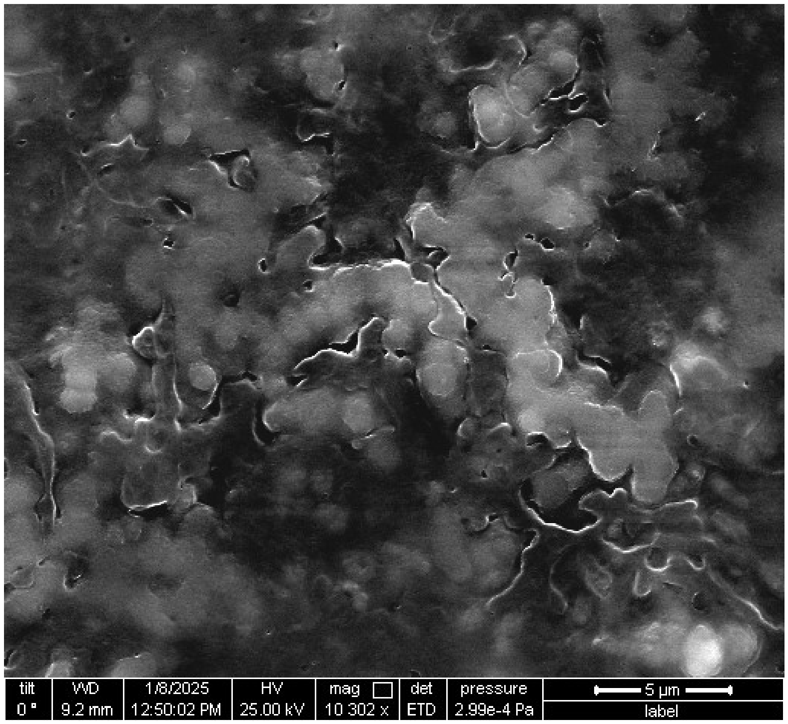

Supplementary Figure S2: Scanning Electron Microscopy (SEM) image of the turmeric film. The image reveals large grain structures, which are consistent with the surface morphology observed in the corresponding Atomic Force Microscopy (AFM) image.

Supplementary Figure 3

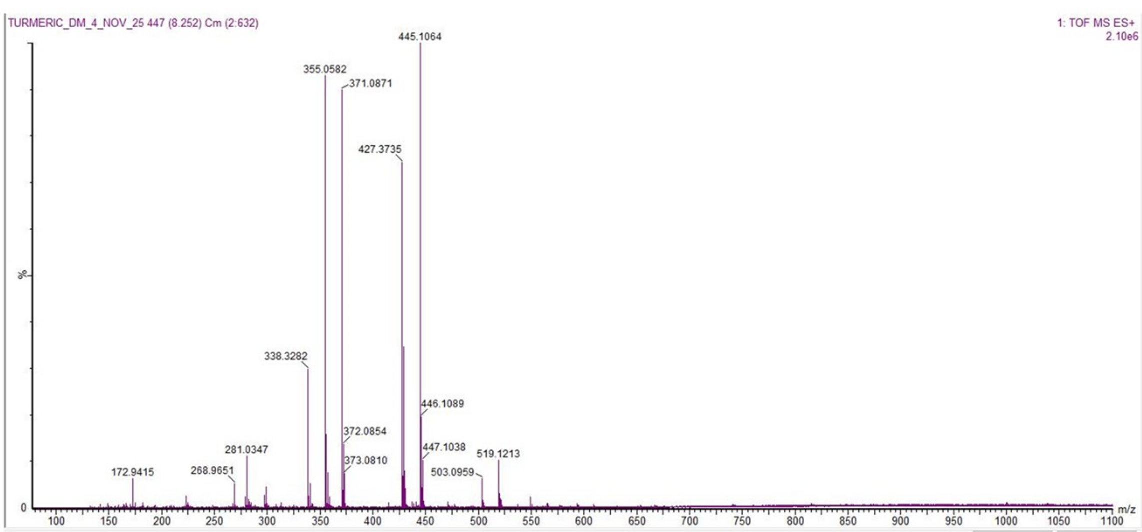

Supplementary Figure 3: The LCMS spectrum of turmeric displays multiple peaks corresponding to its major constituents. Mass spectrometric analysis revealed peaks ranging from m/z 172.9415 to 519.1213, corresponding to various chemical constituents of turmeric. A prominent peak observed at m/z 445.1064 ($[M_1–H+2K]^+$, 100%) along with peaks at m/z 427.3735 ($[M_1–H_2O–H+2K]^+$, 75%) and m/z 338.3282 ($[M_1–OCH_3+H]^+$, 30%) indicate the presence of curcumin. Additionally, a strong peak at m/z 371.0871 ($[M_2+H]^+$, 90%) is attributed to dihydrocurcumin, while the peak at m/z 355.0582 ($[M_3+H–H_2O]^+$, 95%) corresponds to tetrahydrocurcumin.

Supplementary Figure 4

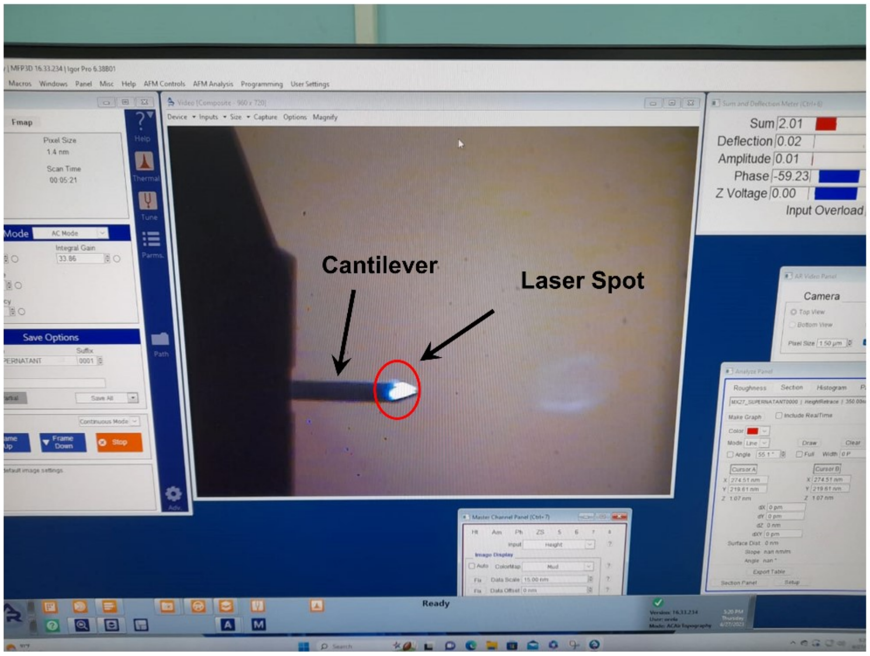

Supplementary Figure S4: The image indicates the laser spot position on the cantilever. To avoid the signal coming from the electrostatic interaction between the sample and cantilever, the laser spot is positioned on the end of the cantilever where the tip is situated.

Supplementary figure 5

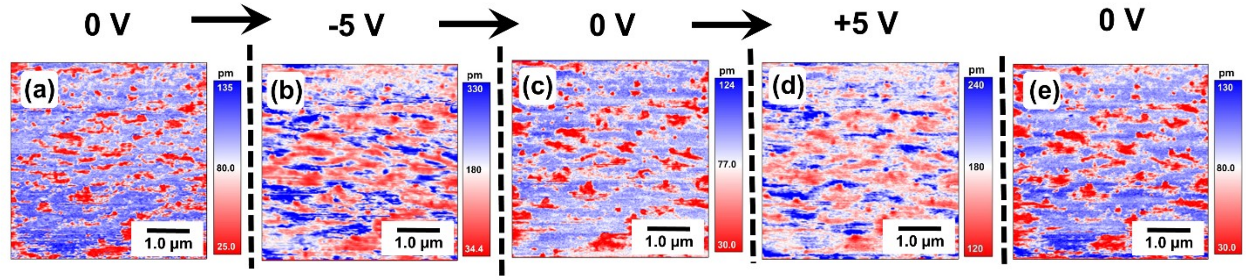

Supplementary Figure S5: PFM amplitude images of turmeric thin film (scan area 5×5 µm) measured in different bias conditions. (a,c,e) represents the PFM amplitude images taken at 0 V tip bias. (b) & (d) indicate PFM amplitude images were taken during negative polling at -5 V and positive polling at +5V. The red and blue areas in the amplitude images suggest that the sample surface is contracted and expanded position.

Supplementary Figure 6

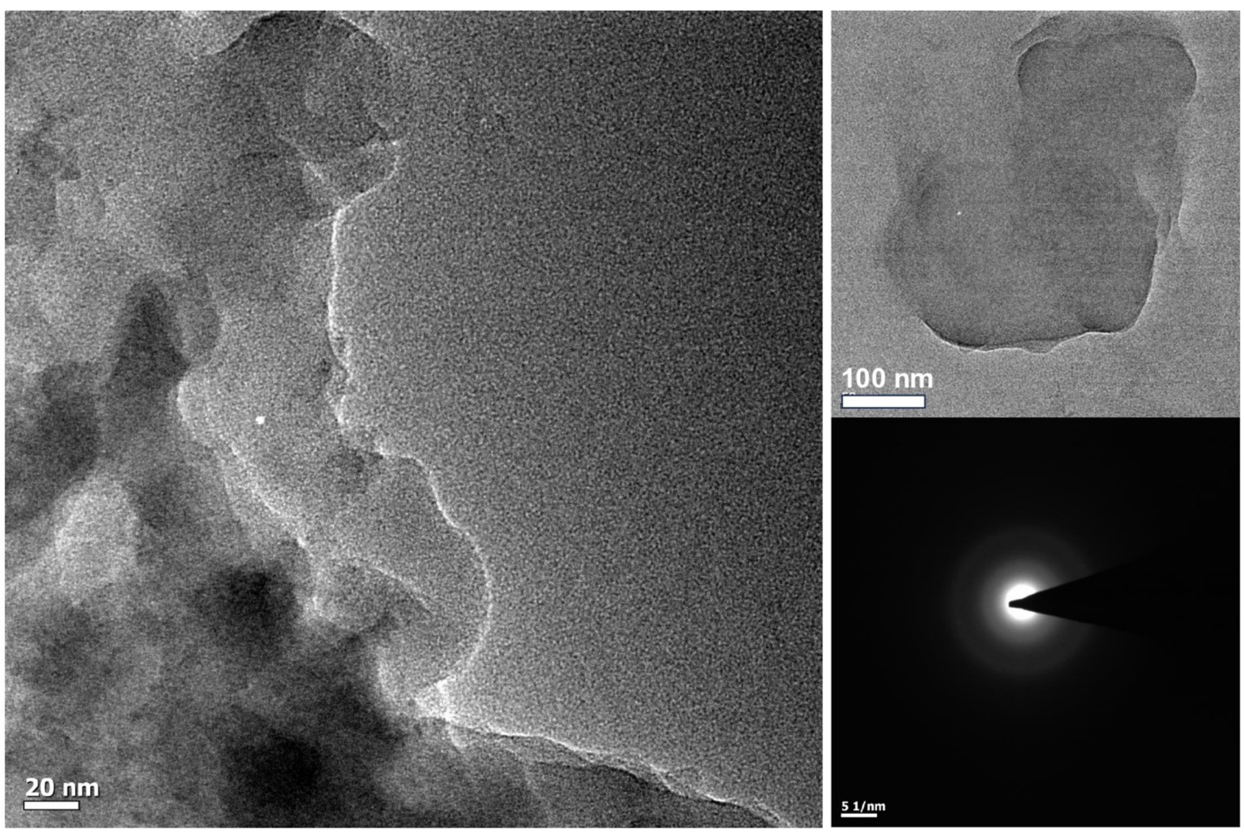

Supplementary Figure S6: The TEM micrographs of the turmeric thin filmis shown, indicate predominantly amorphous morphology with no discernible lattice fringes or crystalline domains, (left panel, scale: 20 nm). The low-magnification image (top right) confirms the formation of continuous thin film regions with irregular edges, while the corresponding Selected Area Electron Diffraction (SAED) pattern (bottom right) displays diffuse concentric rings, further confirming the amorphous nature of the film.

Supplementary figure 7

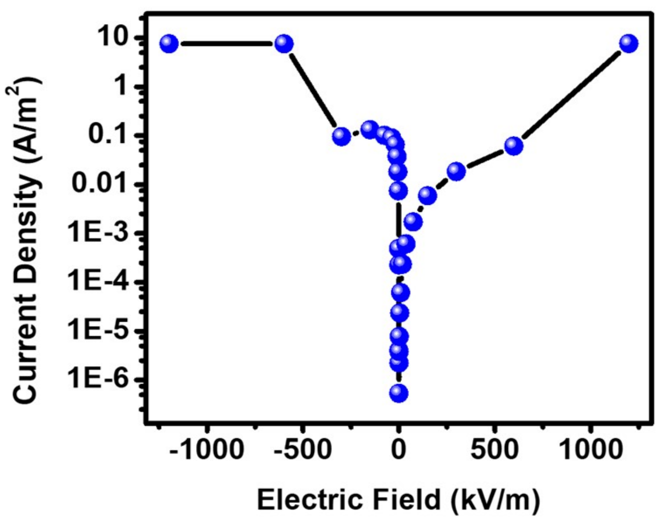

Supplementary Figure S7: Electric field dependent lekeage current density.

Supplementary Figure 8

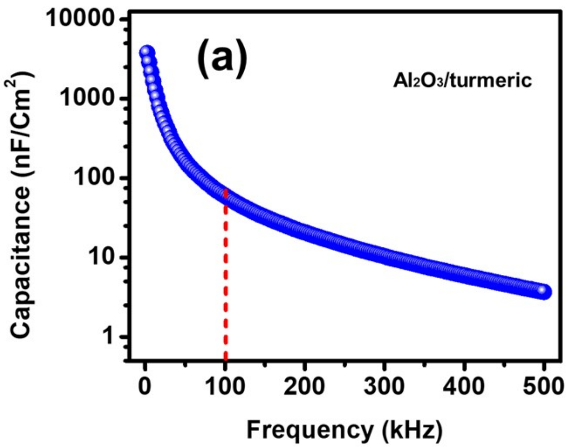

Supplementary Figure S8:

Capacitance vs. Frequency characteristics of the Al_2O_3/Turmeric and turmeric dielectric system are shown in Figure. Capacitor is measured in wide frequency range from 0Hz to 500 kHz. As typically observed in dielectric materials, the capacitance decreases with increasing frequency due to reduced dipolar response at higher frequencies. For field-effect mobility calculations, the capacitance value at 100 kHz was used.

Supplementary Figure 9:

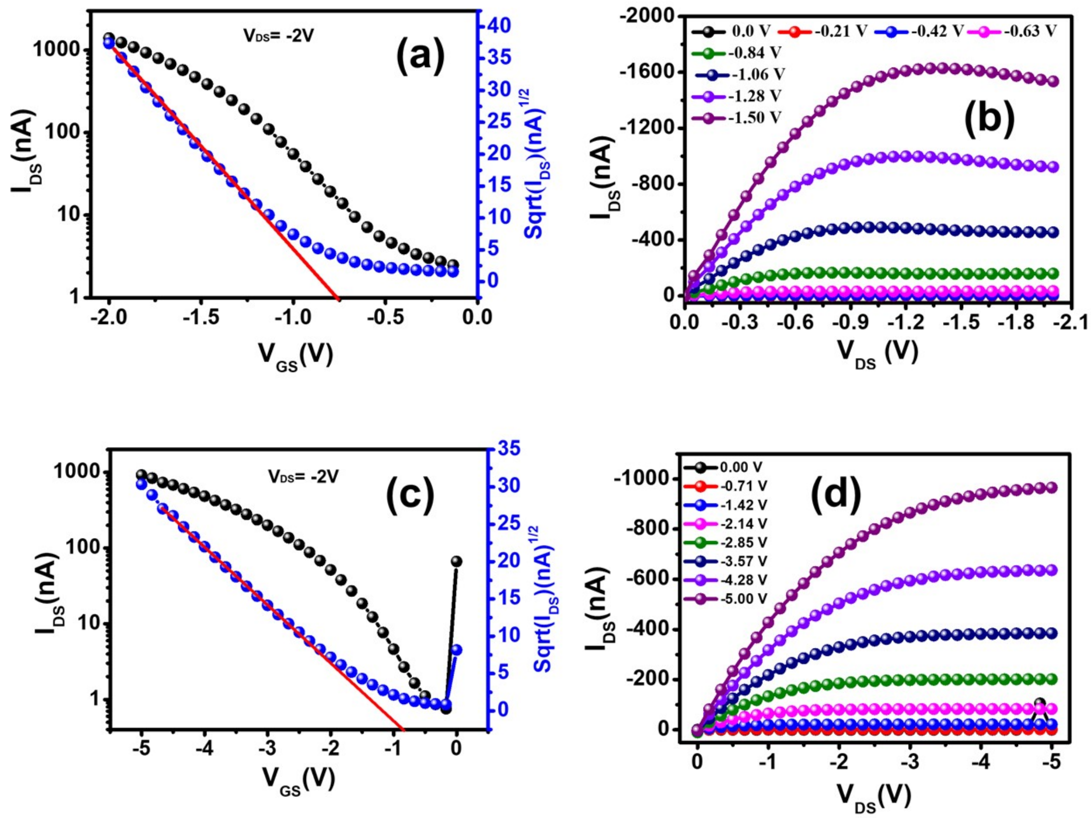

Supplementary Figure S9: The transistor characteristics of OFETs based on Al_2O_3/BTO and Al_2O_3/PMMA bilayer dielectrics are presented in Figure S9. Figures S9a and S59b show the transfer and output characteristics, respectively, of the Al_2O_3/BTO-based transistor. From the transfer characteristics, the field-effect mobility and threshold voltage are calculated to be approximately 0.3 cm^2/Vs and 0.52 V, respectively.

Figures S9c and S9d display the transfer and output characteristics of the Al_2O_3/PMMA-based OFET. In this case, due to the lower dielectric constant of the PMMA layer, the operating voltage increases to –5 V, and the threshold voltage shifts to –0.92 V. The extracted field-effect mobility is approximately 0.015 cm^2/Vs.

Supplementary Figure 10:

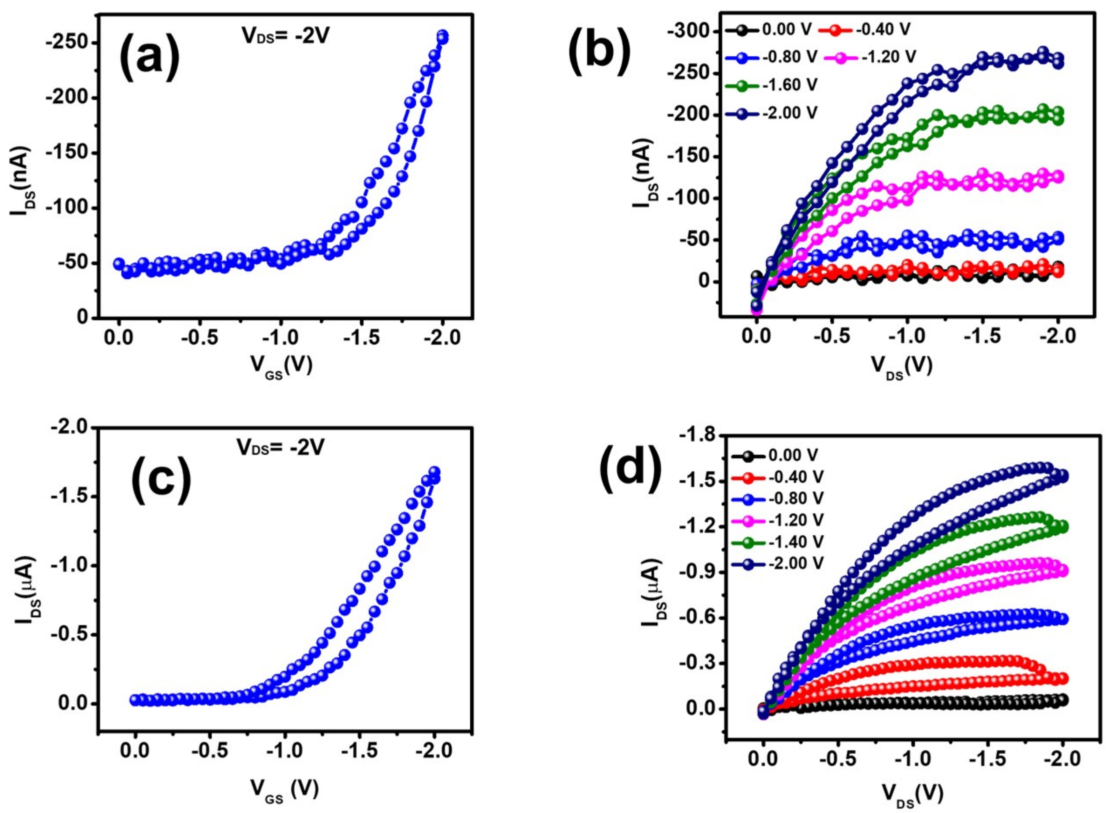

Supplementary Figure S10: The transistor characteristics of OFETs based on only Al_2O_3 and turmeric dielectric layers are presented in Figure S10. Figures S10a and S10b show the transfer and output characteristics, respectively, of the Al_2O_3-based transistor. From the transfer characteristics, the field-effect mobility and threshold voltage are estimated to be 0.039 ± 0.014 cm² /Vs and -1.16 ± 0.12 V, respectively. Figures S10c and S10d display the transfer and output characteristics of the turmeric-based OFET. The corresponding field-effect mobility and threshold voltage are calculated to be 0.25 ± 0.04 cm² /Vs and -0.77 ± 0.13 V, respectively.

Table ST1

Dielectric based Device	Threshold Voltage (V)	Mobility (cm²/V·s)
Al_2O_3	−1.16 ± 0.12	0.039 ± 0.014
Turmeric	−0.77 ± 0.13	0.25 ± 0.04
Al_2O_3/turmeric	−0.15 ± 0.04	0.35 ± 0.03

Supplementary Figure 11:

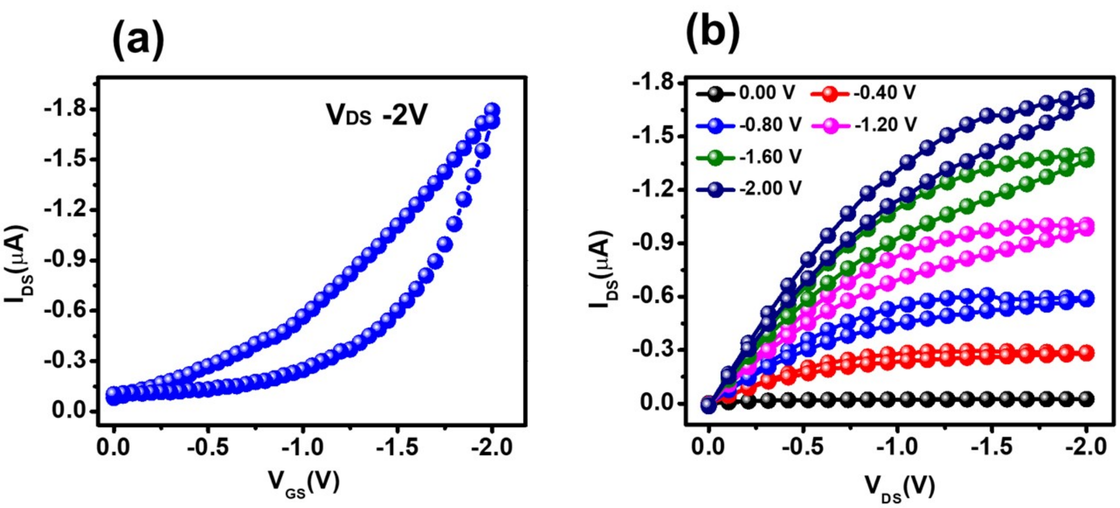

Supplementary Figure S11: The transistor characteristics of OFETs based on Al_2O_3/turmeric dielectric layers are presented in Figure S11. Figures S11a and S11b show the transfer and output characteristics. From the transfer characteristics, the field-effect mobility and threshold voltage are estimated to be 0.31 ± 0.04 cm² /Vs and −0.22 ± 0.21 V, respectively.